Brief Communication | Neuroimaging and Head & Neck

https://doi.org/10.3348/kjr.2018.19.4.783
pISSN 1229-6929 · eISSN 2005-8330
Korean J Radiol 2018;19(4):783-791

Korean Journal of Radiology
KJR

Application of Synthetic MRI for Direct Measurement of Magnetic Resonance Relaxation Time and Tumor Volume at Multiple Time Points after Contrast Administration: Preliminary Results in Patients with Brain Metastasis

Koung Mi Kang, MD[1], Seung Hong Choi, MD, PhD[1-4], Moonjung Hwang, PhD[5], Roh-Eul Yoo, MD[1], Tae Jin Yun, MD[1], Ji-hoon Kim, MD[1], Chul-Ho Sohn, MD[1, 2]

[1]Department of Radiology, Seoul National University Hospital, Seoul 03080, Korea; [2]Department of Radiology, Seoul National University College of Medicine, Seoul 03080, Korea; [3]Institute of Radiation Medicine, Seoul National University Medical Research Center, Seoul 03080, Korea; [4]Center for Nanoparticle Research, Institute for Basic Science (IBS), Seoul 08826, Korea; [5]General Electronics (GE) Healthcare Korea, Seoul 06060, Korea

Objective: The purpose of this study was to investigate the time-dependent effects of contrast medium on multi-dynamic, multi-echo (MDME) sequence in patients with brain metastases.

Materials and Methods: This study included 7 patients with 15 brain metastases who underwent magnetic resonance (MR) examination which included MDME sequences at 1 minute, 10 minutes and 20 minutes after contrast injection. Two volumes of interests, covering an entire tumor (whole tumor) and the enhancing portion of the tumor, were derived from post-contrast synthetic T1-weighted images. Statistical comparisons were performed for three different time delays for histogram parameters of the longitudinal relaxation rate (R_1) and the transverse relaxation rate (R_2), and lesion volumes.

Results: The mean and the median of R_1 and the mean of R_2 in both the whole tumor and the inner enhancing portion were larger on the 10 minutes delayed images than on the 1 minute or 20 minutes delayed images (mean of R_1 in the whole tumor on the 1 minute, 10 minutes, and 20 minutes delayed images: 1.26 ms, 1.39 ms, and 1.37 ms; mean of R_1 in the inner enhancing portion: 1.43 ms, 1.53 ms and 1.44 ms; all $p < 0.017$). The volumes of the whole tumor and the inner enhancing portion were significantly larger in the 10 minutes and 20 minutes delayed images than on the 1 minute delayed images (all $p < 0.017$).

Conclusion: Magnetic resonance relaxation times and the volumes of the whole tumor and the inner enhancing portion were measured larger on the 10 minutes or 20 minutes delayed images than on the 1 minute delayed images. The MDME sequence immediately after contrast injection cannot fully reflect the effects of gadolinium-based contrast agent leakage in the tissue.

Keywords: *Brain tumor; Metastasis; Multi-echo sequence; Quantitative MRI; Contrast-enhanced MRI; Relaxometry*

INTRODUCTION

The novel magnetic resonance imaging (MRI) quantitative sequence, the two-dimensional (2D) fast spin echo (FSE) multi-dynamic, multi-echo (MDME) sequence, enabled the rapid and the simultaneous sampling of physical properties which constitute an magnetic resonance (MR) image (1, 2). The Synthetic MRI from the sequence enables the

Received November 16, 2017; accepted after revision January 19, 2018.
This study was supported by a grant from the Korea Healthcare technology R&D Projects, Ministry for Health, Welfare & Family Affairs (HI16C1111), by the Brain Research Program through the National Research Foundation of Korea (NRF) funded by the Ministry of Science, ICT & Future Planning (2016M3C7A1914002), by Basic Science Research Program through the National Research Foundation of Korea (NRF) funded by the Ministry of Science, ICT & Future Planning (2017R1A2B2006526 and 2017R1A2B2008412), by Creative-Pioneering Researchers Program through Seoul National University (SNU), and by Project Code (IBS-R006-D1).
Corresponding author: Seung Hong Choi, MD, PhD, Department of Radiology, Seoul National University Hospital, 101 Daehak-ro, Jongno-gu, Seoul 03080, Korea.
• Tel: (822) 3668-7832 • Fax: (822) 747-7418 • E-mail: verocay@snuh.org
This is an Open Access article distributed under the terms of the Creative Commons Attribution Non-Commercial License (https://creativecommons.org/licenses/by-nc/4.0) which permits unrestricted non-commercial use, distribution, and reproduction in any medium, provided the original work is properly cited.

Copyright © 2018 The Korean Society of Radiology

production of images with variable contrast-weighting after quantifying the longitudinal relaxation rate (R_1), the transverse relaxation rate (R_2), and the proton density (3, 4). The quantitative values can be directly measured at the same times on the synthetic images with good accuracy and reproducibility (5, 6). Several prior studies using the MDME sequence have investigated the image quality and diagnostic ability of the synthetic MRI (7-11). The applications of MDME sequence in neuroimaging will be further utilized.

The administration of gadolinium-based contrast agent (GBCA) is an important part of MRI in patients with central nervous system (CNS) disease for the diagnosis and monitoring of disease progression. If the integrity of the blood brain barrier (BBB) is changed by a variety of circumstances that increase its permeability, GBCA leaks into the brain tissue (12). GBCA changes the absolute magnetic properties of tissue water, strongly increasing R_1, slightly increases the R_2 and results in hyperintensity on the T1-weighted image (T1WI). This effect may vary with the imaging time after contrast administration. In daily clinical practice, conventional contrast-enhanced MRI is used as a qualitative method that is detected as visible differences based on the signal intensity. Several previous studies investigated post-contrast time-dependent change based on signal intensity on T1WI (13-16). However, absolute signal intensity cannot provide any direct meaning and it should be compared to adjacent normal tissue. On the other hand, tissue relaxometry is a representative quantitative MR technique that can reflect tissue characteristics and reduce the subjectivity of the conventional clinical MRI. Therefore, it has been reported to provide objective measures of tissue properties in variable CNS diseases (17-23). However, because of the prolonged scan time, there has been a limitation in investigating the R_1 and R_2 change, resulting from MR contrast agent.

Development of the new pulse sequence, MDME can provide diverse synthetic images and simultaneous quantification of R_1, R_2, and proton density maps in a scan time of approximately 6 minutes and post-processing time less than 1 minute (6). As the MDME sequence is promising method for the CNS disease, a post-contrast scan has been also applied to patients with multiple sclerosis or brain metastasis (11, 24). However, we could not find a study which applied MDME sequence with different times of image acquisition after contrast injection or evaluated the effects of GBCA on the physical properties of R_1 and R_2 using the MDME sequence. As brain metastasis is the most common intracranial tumor in adults, it is effective to investigate the post-contrast R_1 and R_2 changes in brain metastasis, as a representative CNS pathology that disrupts the BBB.

Therefore, the purpose of this study was to apply the MDME sequence for the direct measurement of MR relaxation times and tumor volumes in brain metastases on synthetic images at different time points after contrast administration and to provide a reference for appropriate imaging time for post-contrast a MDME sequence.

MATERIALS AND METHODS

Study Population

Our Institutional Review Board approved this study protocol, and informed consent was waived. Eight patients with intracerebral metastases, confirmed by imaging follow-up, underwent brain MRI with MDME sequences in June 2014 (15). One patient was excluded due to motion artifacts. Finally, seven patients (four men and three women; mean age, 58 years; age range, 38–66 years) with 15 brain metastases were enrolled in this study. Metastatic brain tumors, which included lung adenocarcinoma (n = 11), renal cell carcinoma (n = 3), and rectal adenocarcinoma (n = 1) were investigated. Mean size of the metastases was 1.85 ± 11.17 cm (range, 0.65–4.72 cm).

MR Examination

All examinations were done using a 3T clinical scanner (Discovery MR750w 3.0T; GE Medical Systems, Milwaukee, WI, USA) with a 32-channel head coil. Quantitative MRI sequences were taken before and after intravenous administration of gadobutrol (Gadovist; Bayer Healthcare, Berlin, Germany) at a dose of 0.1 mmol per kilogram of body weight. The 2D FSE MDME sequence was performed utilizing 4 automatically calculated saturation delays, 2 echo time (TE) of 21.4/85.4 ms and a repetition time (TR) of 4000 ms. All subjects were scanned at the following three different delay time points, after the administration of contrast agent: 1 minute, 10 minutes, and 20 minutes delayed imaging (Fig. 1).

A least square fit was performed on the signal intensity S of each pixel of images per section to calculate the T1, according to the following equation (2):

Korean Journal of Radiology
KJR

$$S = A \times PD \times \exp(-TE / T_2) \times \frac{1 - (1 - \cos[B_1\theta]) \times \exp(-TI/T_1) - \cos(B_1\theta) \times \exp(-TR/T_1)}{1 - \cos(B_1\alpha) \times \cos(B_1\theta) \times \exp(-TR/T_1)}$$

where A is the overall intensity scaling factor considering the coil sensitivity, the radiofrequency chain amplification and the voxel volume, and the applied excitation flip angle α and saturation pulse angle θ were 90 degrees and 120 degrees, respectively. The B_1 field was included in the fitting algorithm to account for B_1 inhomogeneity. Details of the sequence and the post-processing were described by Warntjes et al. (2).

Synthetic T1WI and T2-weighted image (T2WI) were created by the MDME sequence using a vendor-provided

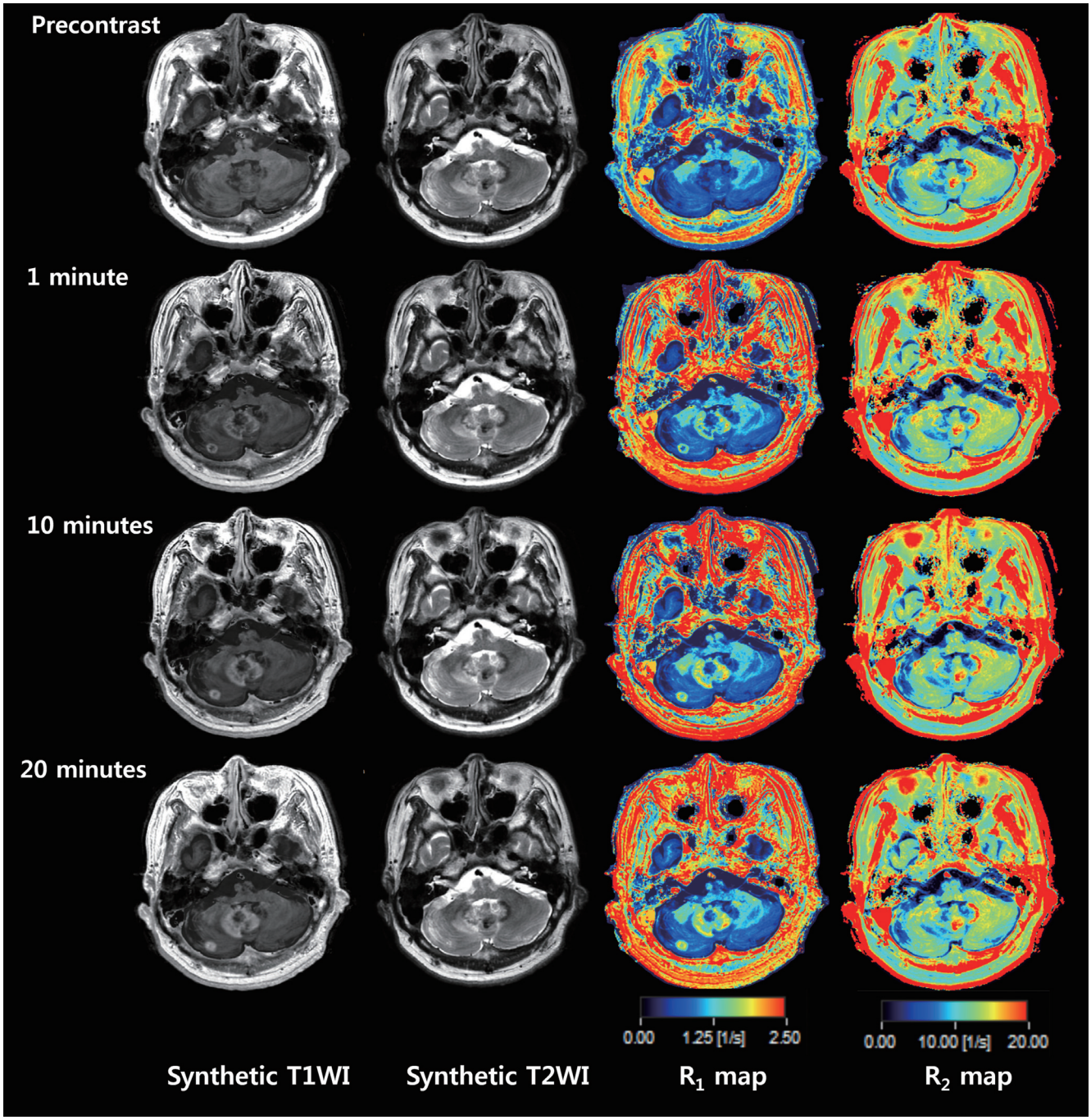

Fig. 1. Representative pre- and post-contrast synthetic T1WI and quantitative R_1 and R_2 maps with different delay times in 63-year-old male patient with brain metastasis. R_1 = longitudinal relaxation rate, R_2 = transverse relaxation rate, T1WI = T1-weighted image, T2WI = T2-weighted image

program (SyMRI7.2; Synthetic MR, Linköping, Sweden). Detailed parameters for the MR sequences are shown in Table 1.

Image Analysis

Quantitative analysis was performed by a radiologist with 8 years of experience in neuroradiology. A lesion was defined as a mass with an abnormal focal parenchymal enhancement with a signal intensity higher than normal brain parenchyma that does not appear as a thin blood vessel on T1WI. R_1 and R_2 values and the volume (mL) of a lesion were measured in a volume of interest (VOI) utilizing a semiautomatic segmentation method in pixel analysis software (Nordic ICE; NordicNeuroLab, Bergen, Norway). Synthetic T1WI of 1 minute, 10 minutes, and 20 minutes delayed imaging were used as structural images for each VOI. A major region of interest (ROI), involving the entire cross-section of a metastasis at its maximum diameter (whole tumor including both the enhancing portion and the nonenhancing necrotic core) was drawn in each section of the three post-contrast synthetic T1WI to derive a VOI. Next, a selective ROI limited to the enhancing portion of the tumor was drawn on each section of the post-contrast synthetic T1WI to derive a VOI representing the enhancing portion of the lesion (Fig. 2). These processes were repeated for different time points and six VOIs were created for each of the lesions. For R_1 and R_2 values of pre-contrast images, synthetic T1WIs of 20 minutes delayed imaging were used as structural reference to define a lesion. Then, a histogram analysis was performed to derive the mean, median, skewness, and kurtosis calculated from the pixel values of a VOI.

Table 1. MDME Sequence Parameters

Acquisition Parameters	Quantitative Sequence (MDME)
TR (ms)	4000
TE (ms)	21.4/85.4
TI (ms)	Automatically calculated 4 different TI
Field of view (cm)	24 x 24
Matrix	320 x 256
Section thickness (mm)	4
Section spacing (mm)	1
Number of sections	20
Flip angle	90
Echo-train length	12
Scan time (min)	5 min, 4 sec

MDME = multi-dynamic, multi-echo, TE = echo time, TI = inversion time, TR = repetition time

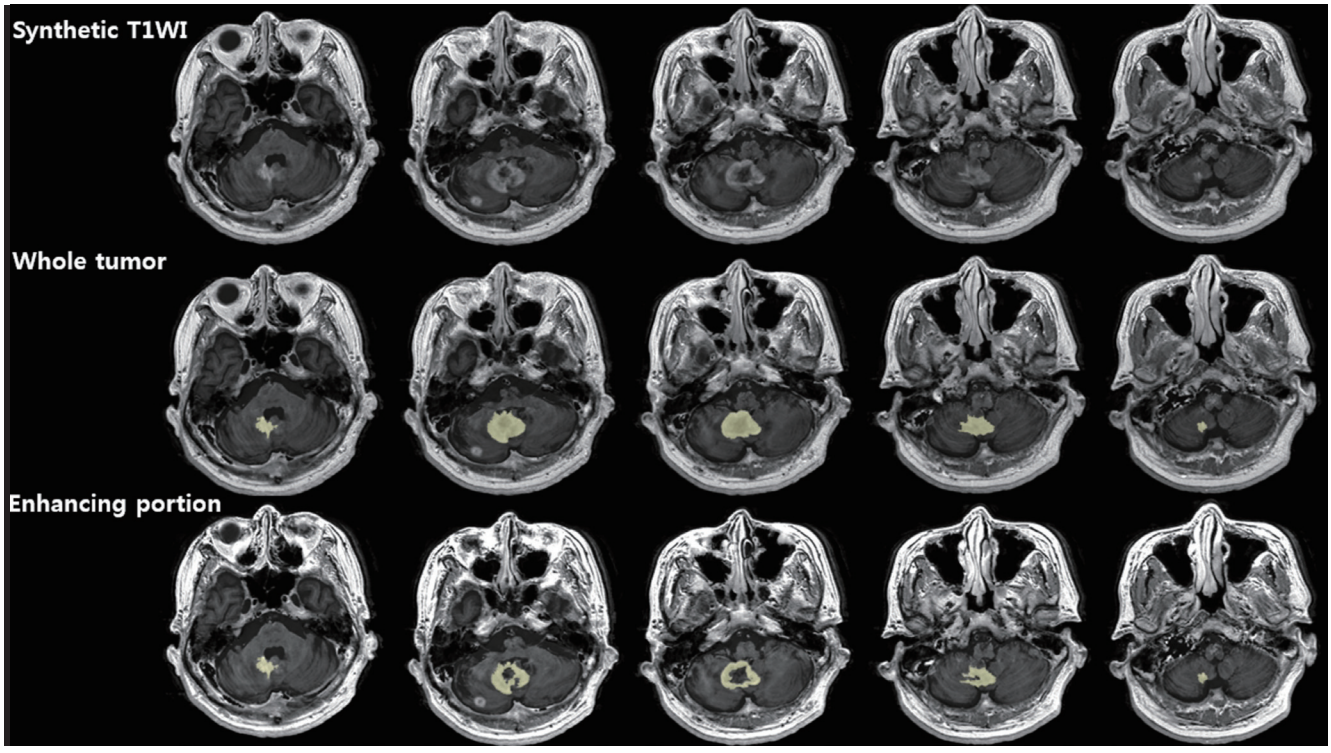

Fig. 2. Post-contrast synthetic T1WI 20 minutes after contrast administration. Regions of interest for entire tumor (second row) and enhancing portion of tumor (third row) to derive volumes of interest.

Korean Journal of Radiology
KJR

Statistical Analysis

The results were reported as median values with the ranges in parentheses. The Friedman test was utilized to evaluate the differences in mean, median, skewness, kurtosis and the lesion volume among the three different time delays (14, 15). Differences were considered significant at $p < 0.05$. For post hoc pairwise multiple comparison, the Wilcoxon signed-rank test was used (1 minute versus 10 minutes delayed images, 1 minute versus 20 minutes delayed images, and 10 minutes versus 20 minutes delayed images). In this case, the Bonferroni-corrected significance level of $p < 0.017$ was used. Statistical analyses were performed using commercially available software (PASW Statistics version 24.0; IBM Corp., Armonk, NY, USA, and MedCalc version 11.1.1.0; MedCalc software, Mariakerke, Belgium).

RESULTS

Both R_1 and R_2 values in the tumor, on the 1 minute delayed images, were significantly elevated compared to the pre-contrast images ($p < 0.001$ for the mean, $p < 0.001$ for the median, skewness and kurtosis).

Longitudinal Relaxation Rate

The Friedman test showed significant differences in R_1 histogram parameters of the whole tumor depending on the three different imaging times (all $p < 0.05$) (Table 2). The post-hoc analyses for whole tumor displayed the mean and median of R_1 were significantly increased on the 10 minutes delayed images compared to the 1 minute delayed images ($p = 0.005$ and $p = 0.002$, respectively) (Fig. 3).

For the enhancing portion of the tumor, significant differences were calculated for the mean of R_1 according to the imaging times (Friedman test, $p = 0.038$). In the post-hoc analyses for the enhancing portion of the tumor, the mean and median R_1 values were significantly larger on the 10 minutes delayed images than on the 20 minutes delayed images ($p = 0.01$ and $p = 0.012$, respectively).

The post-hoc analyses of the skewness and kurtosis of T1 did not show significant difference between the three different imaging times in both whole tumor and enhancing portion of the tumor ($p > 0.017$). The results are summarized in Table 2.

Table 2. Effects of Time Delay after Contrast Injection on Histogram Parameters of Longitudinal Relaxation Rate Values in Brain Metastasis

Parameter	Precontrast	1 Min Delayed Imaging	10 Min Delayed Imaging	20 Min Delayed Imaging	*P* for Friedman Test†	*P* for Post-Hoc Analysis‡		
						1 Min vs. 10 Min	1 Min vs. 20 Min	10 Min vs. 20 Min
Whole tumor								
Mean (ms)	0.61 (0.56, 0.69)	1.26 (1.12, 1.56)	1.39 (1.27, 1.69)	1.37 (1.24, 1.55)	0.047*	0.005*	0.280	0.201
Median (ms)	0.59 (0.55, 0.69)	1.22 (1.09, 1.53)	1.37 (1.27, 1.73)	1.38 (1.30, 1.64)	0.024*	0.002*	0.132	0.629
Skewness	0.71 (0.27, 1.05)	0.37 (-0.07, 0.97)	0.16 (-0.23, 0.72)	0.23 (-0.52, 0.57)	0.022*	0.233	0.088	0.118
Kurtosis	0.29 (-0.09, 6.15)	0.30 (-0.38, 1.99)	0 (-0.52, 0.48)	0.06 (-0.47, 0.55)	0.038*	0.173	0.173	1.000
Enhancing portion of tumor								
Mean (ms)		1.43 (1.30, 1.60)	1.53 (1.45, 1.72)	1.44 (1.32, 1.56)	0.038*	0.053	0.711	0.010*
Median (ms)		1.36 (1.28, 1.56)	1.54 (1.39, 1.73)	1.44 (1.32, 1.55)	0.057	0.017	0.887	0.012*
Skewness		0.72 (0.08, 1.14)	0.34 (0, 0.70)	0.40 (0.06, 0.63)	0.420	0.156	0.191	0.570
Kurtosis		1.21 (-0.31, 2.31)	-0.06 (-0.41, 0.68)	-0.30 (-0.57, 0.20)	0.085	0.031	0.088	0.532

Data are median values with IQRs in parentheses. *Significant *p* value for each test, †For Friedman tests, $p < 0.05$ was considered significant difference, ‡In post-hoc analyses, Bonferroni-corrected significance level of $p < 0.017$ was used. IQRs = interquartile ranges

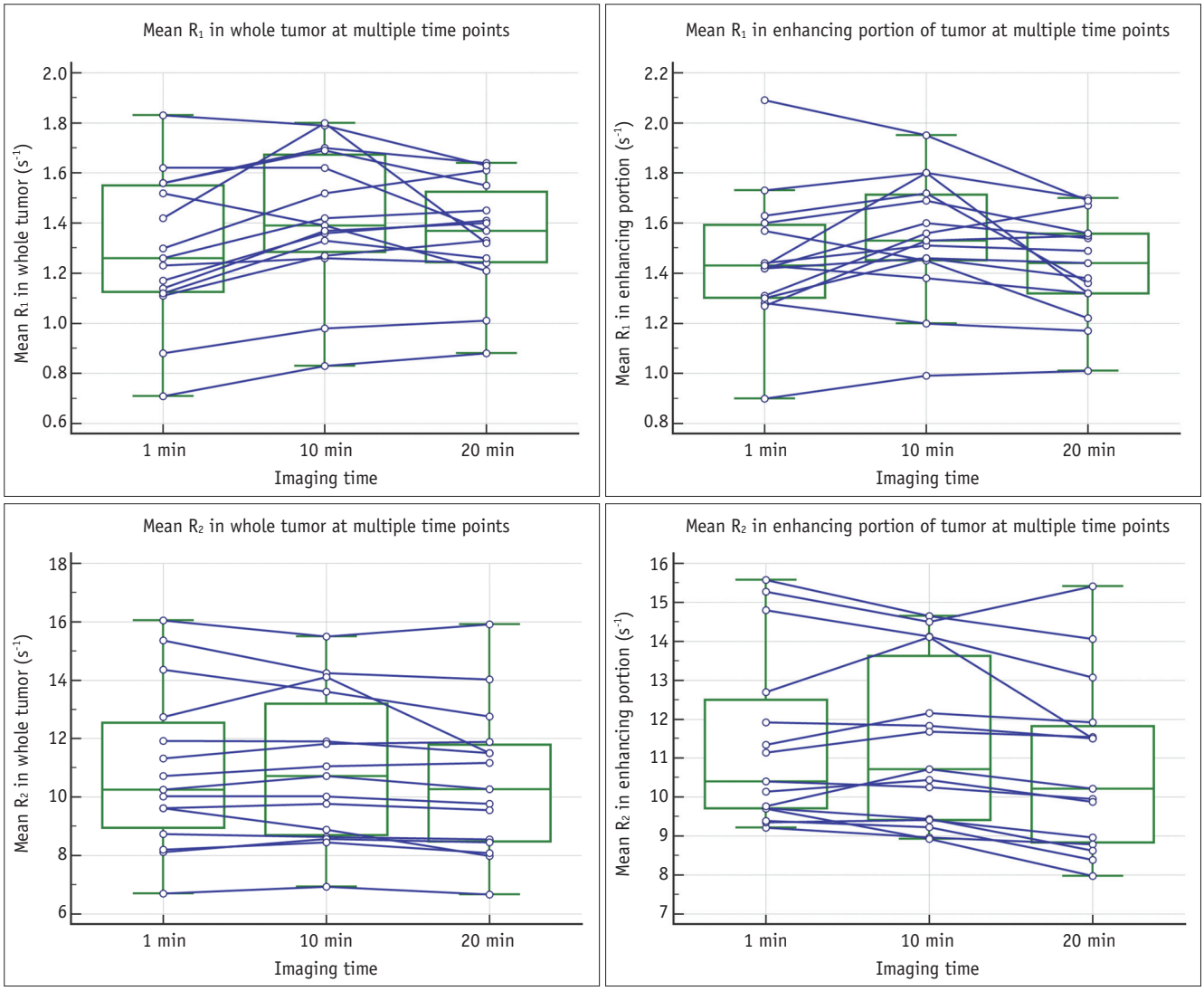

Fig. 3. Box and whisker plots display distribution of mean R_1 and R_2 in whole tumor and enhancing portion of tumor, respectively.
Central box represents values from lower to upper quartile (25–75 percentile). Middle line represents median. Horizontal line extends from minimum to maximum value, excluding outside and far out values that are displayed as separate points.

Transverse Relaxation Rate

In the whole tumor, the mean R_2 was significantly different according to the three different imaging delay times (Friedman test, $p = 0.038$). The other parameters were not significantly altered depending on the imaging times (Friedman test, all $p > 0.05$) (Table 3). In the post-hoc analyses for the whole tumor, the mean of R_2 showed a significant decrease on the 20 minutes delayed images as compared to the 10 minutes delayed images ($p = 0.011$) (Fig. 3).

For the enhancing portion of the tumor, the mean and median of the pixel values were significantly different in R_2 for the three time delays (Friedman test, $p = 0.007$ for both the mean and median). In the post-hoc analyses for the enhancing portion of the tumor, the mean and the median of R_2 were much larger on the 10 minutes delayed images as compared to the 20 minutes delayed images ($p = 0.006$ for the mean and $p = 0.002$ for the median). The results are summarized in Table 3.

Volume

There was a significant difference in the volume of whole tumor for the three different imaging times ($p = 0.022$). The median values of the volume of whole tumor, according to the imaging time, were 0.43 mL (interquartile range [IQR], 0.18–2.67 mL) on the 1 minute delayed images, 0.59 mL (IQR, 0.21–3.09 mL) on the 10 minutes delayed images and 0.71 mL (IQR, 0.26–3.50 mL) on the 20 minutes delayed images. In the post hoc analysis with Wilcoxon signed-rank

Korean Journal of Radiology
KJR

Table 3. Effects of Time Delay after Contrast Injection on Histogram Parameters of Transverse Relaxation Rate Values in Brain Metastasis

Parameter	Precontrast	1 Min Delayed Imaging	10 Min Delayed Imaging	20 Min Delayed Imaging	*P* for Friedman Test†	*P* for Post Hoc Analysis‡		
						1 Min vs. 10 Min	1 Min vs. 20 Min	10 Min vs. 20 Min
Whole tumor								
Mean (ms)	9.88 (7.52, 11.78)	10.26 (8.74, 12.75)	10.72 (8.64, 13.61)	10.28 (8.46, 11.89)	0.038*	0.820	0.088	0.011*
Median (ms)	9.92 (7.46, 11.06)	9.88 (8.87, 13.37)	10.00 (8.87, 13.89)	11.01 (8.74, 12.08)	0.337	0.826	0.320	0.048
Skewness	0.73 (0.08, 1.06)	0.14 (-0.66, 0.59)	0.13 (-0.32, 0.87)	0.29 (-0.24, 0.77)	0.627	0.570	0.820	0.589
Kurtosis	0.18 (-0.38, 2.29)	-0.24 (-0.55, 0.46)	0.10 (-0.39, 0.61)	-0.15 (-0.37, 2.19)	0.549	0.233	0.334	0.349
Enhancing portion of tumor								
Mean (ms)		10.40 (9.71, 12.69)	10.72 (9.41, 14.11)	10.22 (8.79, 11.92)	0.007*	0.865	0.031	0.006*
Median (ms)		10.37 (9.51, 13.30)	10.20 (9.40, 14.04)	9.84 (8.74, 12.08)	0.007*	0.887	0.020	0.002*
Skewness		0.16 (-0.37, 0.48)	0.21 (-0.23, 0.57)	0.29 (-0.18, 0.68)	0.591	0.594	0.733	0.910
Kurtosis		0.04 (-0.51, 0.64)	0.38 (-0.27, 0.84)	0 (-0.51, 0.82)	0.420	0.609	0.609	0.570

Data are median values with IQRs in parentheses. *Significant *p* value for each test, †For Friedman tests, $p < 0.05$ was considered significant difference, ‡In post-hoc analyses, Bonferroni-corrected significance level of $p < 0.017$ was used.

tests conducted with a Bonferroni correction, there were significant increases in the volume of whole tumor on the 10 minutes and 20 minutes delayed images as compared to the 1 minute delayed images ($p = 0.001$ and $p = 0.002$, respectively). There was no significant difference between the 10 minutes and 20 minutes delayed images ($p = 0.028$).

The volume of the enhancing portion of tumor also showed a statistically significant difference for the three different imaging times ($p < 0.001$). The median values for the volume of the enhancing portion of the tumor, according to the imaging time were 0.29 mL (IQR, 0.12–1.73 mL) on the 1 minute delayed images, 0.54 mL (IQR, 0.13–2.61 mL) on the 10 minutes delayed images and 0.69 mL (IQR, 0.21–3.37 mL) on the 20 minutes delayed images. In the post hoc analysis, the volume of the enhancing portion of the tumor revealed a significant increase with the delayed imaging time (both $p = 0.001$ between the 1 minute and 10 minutes delayed images and between the 1 minute and 20 minutes delayed images and $p = 0.01$ between the 10 minutes and 20 minutes delayed images).

DISCUSSION

Quantitative relaxometry can be utilized to obtain fundamental and absolute information on tissue properties (22). As recently introduced synthetic MRI enabled direct measurement of R_1 and R_2 values within a reasonable time, we applied the sequences to investigate the time-dependent changes of R_1 and R_2 on the post-contrast MRI and measured them in brain metastases at three delay time points. We observed the mean of R_1 and R_2 in the whole tumor were higher on the 10 minutes delayed images than on the 1 minute delayed images. For the enhancing portion of the tumor, the mean and the median of R_1 and the mean of R_2 were higher on the 10 minutes delayed images than on the 20 minutes delayed images. Therefore, R_1 and R_2 values measured on the synthetic MRI were significantly changed at 10 minutes after contrast injection. In addition, we observed that volumes of the whole tumor and the inner enhancing portion were significantly larger at the 10 minutes delayed images as compared to the 1 minute delayed images.

There have been a few studies that reported the time

dependent changes of MR relaxation times. We found a previous study which investigated time-dependent changes in the local T1 relaxation time (T1) in variable brain tumors after the intravenous injection of GBCA, using a magnetic focusing technique (25). T1 values of the tumors were measured serially for 60 minutes, and most values of T1 reached the minimal values at 5 minutes or, at latest, 10 minutes after the injection of GBCA (25). Similar to these results, our study the using synthetic MRI also revealed that measured MR relaxation times on the delayed scan were significantly different from those on the immediate post-contrast scan. In addition, we included the skewness and kurtosis in the analyses because they are biomarkers for tumor heterogeneity (26-29). Although Friedman test revealed that the skewness and kurtosis of R_1 for the whole tumor were significantly different according to the different imaging delay times, their differences were attenuated in the post-hoc analyses. Based on our findings and previous knowledge, post-contrast quantitative MRI needs to be acquired at least 5 minutes after contrast injection to reflect enough changes in MR relaxation times.

The measurability of a disease is important for the assessment of response in patients with malignant tumors who are given anticancer treatments. In our study, two kinds of volumes for the whole tumor (including enhancing portion and nonenhancing necrotic core) and the inner enhancing portion were significantly larger on the 10 minutes and 20 minutes delayed images as compared to the 1 minute delayed images. Whereas no significant difference was observed between the 10 minutes and 20 minutes delayed images in the whole tumor, the volume of the enhancing portion of the tumor was larger on the 20 minutes delayed images than the 10 minutes delayed images. Our results are similar to a few previous reports, which showed the lesion contrast from signal intensities improved with delayed imaging time (13, 14). As the post-contrast synthetic T1WIs were used as structural images for each VOI, we could indirectly validate the time-dependent changes in tumor volume measured by the MDME sequence as compared to the conventional MR imaging.

Post-contrast synthetic MRI could demonstrate the R_1 and the R_2 changes caused by GBCA leakage in the brain metastasis. By using synthetic MRI, the changed MR relaxation times were easily and directly measured and compared between pre- and post-contrast scans. In addition, the changes were much larger on the delayed scan rather than 1 minute delayed scan. Even though these results are predictable, there has been no prior study, which put a theory on the synthetic MRI. Therefore, this preliminary study is meaningful as a reference for future studies using post-contrast synthetic MRI.

The current study has several limitations. First, the number of patients was small. Because of the limitation of the acquisition time, it was difficult to obtain MDME sequences four times in many of these patients. Second, in the case of multiple lesions in the same patient, each lesion was regarded as an independent lesion. In addition, the constitution of sample was heterogeneous, and the pathology of metastases might have affected the time-dependent changes in tissue relaxation. However, our purpose was not to differentiate the pathology of metastases, but to analyze the time-dependent effects of the contrast medium on MDME sequence in an enhancing mass. We could obtain reliable results by studying various histogram parameters and statistical verification. Third, our study did not investigate time-dependent changes of R_1 and R_2 with a shorter interval of imaging time delays. This was also caused by the limitation of acquisition time. In addition, it took 5 minutes and 4 seconds to acquire a MDME sequence, the time interval used in our study seems to be applicable for investigating the time-dependent changes of tissue relaxation times in brain metastasis.

In conclusion, the MDME sequence immediately after contrast injection cannot fully reflect the effects of GBCA leakage in a tissue. Both the changes in the MR relaxation times and the volume of a tumor were larger on the 10 minutes or 20 minutes delayed images rather than on the 1 minute delayed images. As the post-contrast synthetic MRI can provide objective change of tissue properties related to contrast leakage in various CNS diseases, its application in neuroimaging will be further expanded. Our results may provide a reference for appropriate imaging time for post-contrast MDME sequence.

REFERENCES

1. Warntjes JB, Dahlqvist O, Lundberg P. Novel method for rapid, simultaneous T1, T2*, and proton density quantification. *Magn Reson Med* 2007;57:528-537
2. Warntjes JB, Leinhard OD, West J, Lundberg P. Rapid magnetic resonance quantification on the brain: optimization for clinical usage. *Magn Reson Med* 2008;60:320-329
3. Riederer SJ, Suddarth SA, Bobman SA, Lee JN, Wang HZ, MacFall JR. Automated MR image synthesis: feasibility studies. *Radiology* 1984;153:203-206

4. Bobman SA, Riederer SJ, Lee JN, Suddarth SA, Wang HZ, Drayer BP, et al. Cerebral magnetic resonance image synthesis. *AJNR Am J Neuroradiol* 1985;6:265-269
5. Krauss W, Gunnarsson M, Andersson T, Thunberg P. Accuracy and reproducibility of a quantitative magnetic resonance imaging method for concurrent measurements of tissue relaxation times and proton density. *Magn Reson Imaging* 2015;33:584-591
6. Vågberg M, Ambarki K, Lindqvist T, Birgander R, Svenningsson A. Brain parenchymal fraction in an age-stratified healthy population - determined by MRI using manual segmentation and three automated segmentation methods. *J Neuroradiol* 2016;43:384-391
7. Blystad I, Warntjes JB, Smedby O, Landtblom AM, Lundberg P, Larsson EM. Synthetic MRI of the brain in a clinical setting. *Acta Radiol* 2012;53:1158-1163
8. Ambarki K, Lindqvist T, Wåhlin A, Petterson E, Warntjes MJ, Birgander R, et al. Evaluation of automatic measurement of the intracranial volume based on quantitative MR imaging. *AJNR Am J Neuroradiol* 2012;33:1951-1956
9. Warntjes JB, Engström M, Tisell A, Lundberg P. Brain characterization using normalized quantitative magnetic resonance imaging. *PLoS One* 2013;8:e70864
10. West J, Aalto A, Tisell A, Leinhard OD, Landtblom AM, Smedby Ö, et al. Normal appearing and diffusely abnormal white matter in patients with multiple sclerosis assessed with quantitative MR. *PLoS One* 2014;9:e95161
11. Hagiwara A, Hori M, Suzuki M, Andica C, Nakazawa M, Tsuruta K, et al. Contrast-enhanced synthetic MRI for the detection of brain metastases. *Acta Radiol Open* 2016;5:2058460115626757
12. Essig M, Weber MA, von Tengg-Kobligk H, Knopp MV, Yuh WT, Giesel FL. Contrast-enhanced magnetic resonance imaging of central nervous system tumors: agents, mechanisms, and applications. *Top Magn Reson Imaging* 2006;17:89-106
13. Healy ME, Hesselink JR, Press GA, Middleton MS. Increased detection of intracranial metastases with intravenous Gd-DTPA. *Radiology* 1987;165:619-624
14. Uysal E, Erturk SM, Yildirim H, Seleker F, Basak M. Sensitivity of immediate and delayed gadolinium-enhanced MRI after injection of 0.5 M and 1.0 M gadolinium chelates for detecting multiple sclerosis lesions. *AJR Am J Roentgenol* 2007;188:697-702
15. Jeon JY, Choi JW, Roh HG, Moon WJ. Effect of imaging time in the magnetic resonance detection of intracerebral metastases using single dose gadobutrol. *Korean J Radiol* 2014;15:145-150
16. Bae MS, Jahng GH, Ryu CW, Kim EJ. A systematically designed study to investigate the effects of contrast medium on diffusion tensor MRI. *J Neuroradiol* 2011;38:214-222
17. Bernasconi A, Bernasconi N, Caramanos Z, Reutens DC, Andermann F, Dubeau F, et al. T2 relaxometry can lateralize mesial temporal lobe epilepsy in patients with normal MRI. *Neuroimage* 2000;12:739-746
18. Hasan KM, Walimuni IS, Abid H, Wolinsky JS, Narayana PA. Multi-modal quantitative MRI investigation of brain tissue neurodegeneration in multiple sclerosis. *J Magn Reson Imaging* 2012;35:1300-1311
19. Neema M, Stankiewicz J, Arora A, Dandamudi VS, Batt CE, Guss ZD, et al. T1- and T2-based MRI measures of diffuse gray matter and white matter damage in patients with multiple sclerosis. *J Neuroimaging* 2007;17 Suppl 1:16S-21S
20. Mamere AE, Saraiva LA, Matos AL, Carneiro AA, Santos AC. Evaluation of delayed neuronal and axonal damage secondary to moderate and severe traumatic brain injury using quantitative MR imaging techniques. *AJNR Am J Neuroradiol* 2009;30:947-952
21. Waldman AD. Magnetic resonance imaging of brain tumors-time to quantify. *Discov Med* 2010;9:7-12
22. Cheng HL, Stikov N, Ghugre NR, Wright GA. Practical medical applications of quantitative MR relaxometry. *J Magn Reson Imaging* 2012;36:805-824
23. Højrup S, Jensen FT, Hokland S, Simonsen C, Christensen T, Frøkiærb J, et al. Interobserver and within-subject variances of T_2-relaxation time and ^{1}H-metabolite ratios in the normal hippocampus. *J Neuroradiol* 2007;34:198-204
24. Warntjes JB, Tisell A, Landtblom AM, Lundberg P. Effects of gadolinium contrast agent administration on automatic brain tissue classification of patients with multiple sclerosis. *AJNR Am J Neuroradiol* 2014;35:1330-1336
25. Yoshida K, Furuse M, Kaneoke Y, Saso K, Inao S, Motegi Y, et al. Assessment of T_1 time course changes and tissue-blood ratios after Gd-DTPA administration in brain tumors. *Magn Reson Imaging* 1989;7:9-15
26. Just N. Histogram analysis of the microvasculature of intracerebral human and murine glioma xenografts. *Magn Reson Med* 2011;65:778-789
27. Baek HJ, Kim HS, Kim N, Choi YJ, Kim YJ. Percent change of perfusion skewness and kurtosis: a potential imaging biomarker for early treatment response in patients with newly diagnosed glioblastomas. *Radiology* 2012;264:834-843
28. Downey K, Riches SF, Morgan VA, Giles SL, Attygalle AD, Ind TE, et al. Relationship between imaging biomarkers of stage I cervical cancer and poor-prognosis histologic features: quantitative histogram analysis of diffusion-weighted MR images. *AJR Am J Roentgenol* 2013;200:314-320
29. Woo S, Cho JY, Kim SY, Kim SH. Histogram analysis of apparent diffusion coefficient map of diffusion-weighted MRI in endometrial cancer: a preliminary correlation study with histological grade. *Acta Radiol* 2014;55:1270-1277